Postprint of: Czyżniewski M., Łangowski R., Klassa D., Matwiszyn M., A case study of robust sliding mode control applied to inverted pendulum on a cart, 25th International Conference on Methods and Models in Automation and Robotics (MMAR), 2021, pp. 156-161, DOI: 10.1109/MMAR49549.2021.9528458

A case study of robust sliding mode control applied to inverted pendulum on a cart

Mateusz Czyżniewski, Rafał Łangowski, Dawid Klassa, Mateusz Matwiszyn
Department of Electrical Engineering, Control Systems and Informatics, Gdańsk University of Technology
ul. G. Narutowicza 11/12, 80-233 Gdańsk, Poland
Email: mateusz.czyzniewski@pg.edu.pl, rafal.langowski@pg.edu.pl

***Abstract*—A control problem of an inverted pendulum on a cart has been addressed in this paper. In particular, a synthesis of alternative sliding mode control for stabilisation of an inverted pendulum at an upper equilibrium point has been investigated. Hence, the feasibility of implementing the developed control system, taking into account primarily the friction of the cart against the gantry and the limited length of the gantry, in a real plant has been given. The proposed control system has been tested by simulation in Matlab/Simulink environment and satisfactory performance of its operation has been obtained.**

I. Introduction

An inverted pendulum on a cart (linear inverted pendulum – IP) is one of the widespread benchmarks of non–linear and under–actuated systems, which are characterised by non–minimal phase as well as chaotic behaviour, and sensitiveness of parameters uncertainty [1], [2]. Thus, an IP is used as a popular application for a synthesis of control systems, and estimation purposes. The main goal of an IP control is its stabilisation at an upper equilibrium point (upper position), and often lifting up a pendulum arm to the neighbourhood of this position (swing–up mechanism). Taking into account the above–mentioned features of an IP, designing a relevant control system is a challenging task. This causes many approaches to solving the IP control problem to be found in the literature. These include approaches using separate controllers to swing–up a pendulum arm and its stabilisation at the upper position completed by a switching condition between regulators as well as a single controller, which is able to realise both phases. In the first group, for example, various configurations of PID controllers [3], [4], state–feedback–based controllers [3], [5], [6] or sliding mode control techniques (SMC) [7]–[10] are used to the IP stabilisation. Whereas, typically the swing–up mechanism and switching condition are based on well established energetic approach [2], [10], [11]. In turn, the second group includes methods using SMC [7], fuzzy control strategy [12] or neural networks [13]. In the further part of the paper, a control system consisting of SMC and swing–up mechanism (SU) with switching condition (SC) is considered. In general, SMC is very often associated with preceding non–linear coordinate transformation, due to obtaining controllability canonical form [14], [15]. Hence, SMC is synthesised by utilising approximated feedback linearisation based on the change of coordinate [10], [16], [17].

The main aim of this paper is the synthesis of a robust, (hybrid) control system, which includes SMC for upper position stabilisation and SU with SC. However, the focus has been primarily on stabilising the IP using SMC. Thus, the main topic is to establish the sliding mode algorithm, robust to external disturbances and uncertainties in internal dynamics. Compared to the work performed in, e.g., [8]–[10], provided a synthesis of the control system for a more sophisticated IP mathematical model. More specifically, the IP model includes the friction phenomenon of the cart against the gantry and expanded the IP geometry by adding a load to the end of the pendulum's arm [2]. Therefore, to develop the invoked methodology, an extended analysis of the IP model for the control system synthesis purposes, and a different transformation of coordinate are investigated. Moreover, the analysis of the usage of approximation system is more extended than in [8]–[10]. Also, during simulations, the actuator with control signal saturation and sensor subsystems are considered. It is because the devised control system should potentially be implementable in a real plant from [2].

The paper is organised as follows. Section II includes the problem formulation. The analysis of the IP model from the point of view of control system design needs is presented in section III. In section IV the synthesis of the IP control system is given. Next, simulation results are described in section V. The paper is concluded in section VI.

II. Problem formulation

The considered IP is illustrated in Fig. 1 [2]. This IP is composed of the following elements. The cart is mounted to the gantry consisting of two guide shafts. The arm is mounted on the cart at the joint. The arm includes two elements, i.e., the rod and the load. The IP is fastened on a supporting element, so–called the base. The particular symbols in Fig. 1 stand for: $\Theta(t)$ - angular displacement of the pendulum arm; $s(t)$ - linear displacement of the cart; $Z(t) \in \boldsymbol{\mathcal{Z}} \subset \mathbb{R}$ - external disturbance (uncontrolled force) applied to the pendulum arm; $F(t) \in \boldsymbol{\mathcal{F}} \subset \mathbb{R}$ - force (control signal) applied to the cart; $T(t) \in \boldsymbol{\mathcal{T}} \subset \mathbb{R}$ - friction force between the cart and the gantry; m_{c} - mass of the load; m_{p} - mass of the rod; m_{w} - mass of the cart.

As already mentioned, the main purpose of this paper is to design SMC to stabilise the IP at an upper equilibrium point. Clearly, the operation of control system is desired to

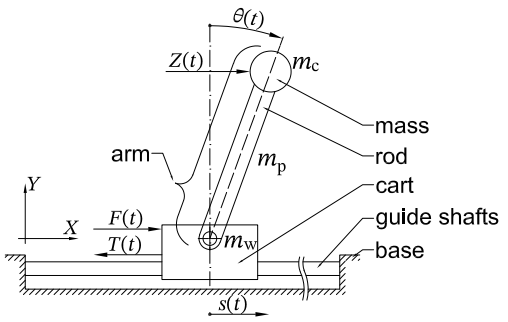

Fig. 1. Graph of the considered IP [2].

stabilise the IP at the upper position (starting from the bottom position, i.e. $\boldsymbol{x}_{\mathrm{down}} = \begin{bmatrix}0 & 0 & 0 & \pm\pi\end{bmatrix}^{\mathrm{T}} \in \boldsymbol{\mathcal{X}} \subset \mathbb{R}^4$), and also placing the cart in the middle of the gantry, which is exactly described as tracking the following operating point $\boldsymbol{x}_{\mathrm{op}} = \begin{bmatrix}0 & 0 & 0 & 0\end{bmatrix}^{\mathrm{T}}$, which is associated with the following vector of state variables $\boldsymbol{x}(t) \in \boldsymbol{\mathcal{X}} \subset \mathbb{R}^4$:

$$\begin{aligned}\boldsymbol{x}(t) &= \begin{bmatrix}s(t) & \dot{s}(t) & \Theta(t) & \dot{\Theta}(t)\end{bmatrix}^{\mathrm{T}} \\ &= \begin{bmatrix}x_1(t) & x_2(t) & x_3(t) & x_4(t)\end{bmatrix}^{\mathrm{T}},\end{aligned} \tag{1}$$

where $\dot{(\cdot)}$ is the derivative with respect to t.

Moreover, the synthesis of the control system includes the external disturbance occurrences ($Z(t)$), and also problem of parametric uncertainty, which is associated with not exactly known mass of the load attached to the end of the pendulum arm, i.e. $\underline{m}_{\mathrm{c}} \leq m_{\mathrm{c}} \leq \overline{m}_{\mathrm{c}}$, where $\underline{m}_{\mathrm{c}}$ and $\overline{m}_{\mathrm{c}}$ are the lower and upper bound of the load mass, respectively. Also, for the design of the control system, it is assumed that all state variables are measurably available (or are estimated). In turn, the actuator consisting of a DC motor with a gearbox is treated as a subsystem of the IP control system, whose dynamics can be neglected (by comparing it with the dynamics of the IP). It is worth adding, however; that in the general case, the actuator's dynamics can significantly affect the performance of the control system. This problem can be solved by using an internal control system in the form of an open–loop proportional regulator or a PID type controller to control the DC motor current.

III. Model of the IP for control system synthesis

It is known that a suitable (utility) IP model is required for SMC synthesis. This model is usually based on a cognitive model that predicts the real behaviour of the IP. In the literature three main approaches to the IP modelling, i.e., via Euler–Lagrange equation, Kane's method, or Newton's laws of motion can be found [18]. In this paper, the model derived in [2] is used, based on the third approach, of the form:

$$\begin{aligned}&\ddot{s}(t)\left[m_{\mathrm{w}}\left(I + m_{\mathrm{r}}l^2\right) + m_{\mathrm{r}}I + m_{\mathrm{r}}^2 l^2 \sin^2\theta(t)\right] = \\ &-\dot{s}(t)k_{\mathrm{T}}\left(I + m_{\mathrm{r}}l^2\right) + m_{\mathrm{r}}l\dot{\theta}^2(t)\left(I + m_{\mathrm{r}}l^2\right)\sin\theta(t) \\ &-0.5\left(m_{\mathrm{c}}l_{\mathrm{c}} + m_{\mathrm{p}}l_{\mathrm{p}}\right)m_{\mathrm{r}}lg\sin\left(2\theta(t)\right), \\ &+F(t)\left(I + m_{\mathrm{r}}l^2\right) \\ &+Z(t)\left[\left(I + m_{\mathrm{r}}l^2\right) - m_{\mathrm{r}}ll_{\mathrm{c}}\cos^2\theta(t)\right]\end{aligned} \tag{2}$$

$$\begin{aligned}&\ddot{\theta}(t)\left[m_{\mathrm{w}}\left(I + m_{\mathrm{r}}l^2\right) + m_{\mathrm{r}}I + m_{\mathrm{r}}^2 l^2 \sin^2\theta(t)\right] = \\ &\left(m_{\mathrm{r}} + m_{\mathrm{w}}\right)\left(m_{\mathrm{c}}l_{\mathrm{c}} + m_{\mathrm{p}}l_{\mathrm{p}}\right)g\sin\theta(t) \\ &+\dot{s}(t)k_{\mathrm{T}}m_{\mathrm{r}}l\cos\theta(t) - 0.5m_{\mathrm{r}}^2 l^2\dot{\theta}^2(t)\sin\left(2\theta(t)\right). \\ &-F(t)m_{\mathrm{r}}l\cos\theta(t) \\ &+Z(t)\left[m_{\mathrm{w}}l_{\mathrm{c}} + m_{\mathrm{r}}\left(l_{\mathrm{c}} - l\right)\right]\cos\theta(t)\end{aligned} \tag{3}$$

where: $\ddot{(\cdot)}$ denotes the second derivative with respect to t; $l_{\mathrm{c}}, l_{\mathrm{p}}$ stand for the distances from the beginning of the arm to centres of gravity of load and rod, respectively, and $l_{\mathrm{c}} = 2l_{\mathrm{p}}$; l is the distance from the beginning of the arm to centre of gravity of the arm, determined by:

$$l = l_{\mathrm{p}}\left(1 + \frac{m_{\mathrm{c}}}{m_{\mathrm{r}}}\right); \tag{4}$$

m_{r} denotes the mass of arm, determined by:

$$m_{\mathrm{r}} = m_{\mathrm{p}} + m_{\mathrm{c}}; \tag{5}$$

I is the moment of inertia for the arm, defined as [2]:

$$I = l_{\mathrm{p}}^2\left[m_{\mathrm{p}}\left(\frac{1}{3} + \frac{m_{\mathrm{c}}^2}{m_{\mathrm{r}}^2}\right) + m_{\mathrm{c}}\frac{m_{\mathrm{p}}^2}{m_{\mathrm{r}}^2}\right]; \tag{6}$$

k_{T} signifies the friction coefficient between the cart and the gantry; g is the gravitational acceleration.

The affine non–linear form of (2) and (3), after introducing the state vector $\boldsymbol{x}(t)$, is as follows [15], [19]:

$$\begin{cases}\dot{x}_1(t) & = x_2(t) \\ \dot{x}_2(t) & = \dfrac{\mathrm{F}_1(\boldsymbol{x}(t))}{\mathrm{D}(\boldsymbol{x}(t))} + \dfrac{\mathrm{B}_1(\boldsymbol{x}(t))}{\mathrm{D}(\boldsymbol{x}(t))}F(t) + \dfrac{\mathrm{G}_1(\boldsymbol{x}(t))}{\mathrm{D}(\boldsymbol{x}(t))}Z(t) \\ \dot{x}_3(t) & = x_4(t) \\ \dot{x}_4(t) & = \dfrac{\mathrm{F}_2(\boldsymbol{x}(t))}{\mathrm{D}(\boldsymbol{x}(t))} + \dfrac{\mathrm{B}_2(\boldsymbol{x}(t))}{\mathrm{D}(\boldsymbol{x}(t))}F(t) + \dfrac{\mathrm{G}_2(\boldsymbol{x}(t))}{\mathrm{D}(\boldsymbol{x}(t))}Z(t) \\ \boldsymbol{x}(t_0) & = \boldsymbol{x}_0\end{cases}, \tag{7}$$

where the smooth vector fields expressions, which mapping from connected and analytical $\boldsymbol{\mathcal{X}}$ to tangent space $T_{\mathrm{x}}\boldsymbol{\mathcal{X}}$, used for dynamics presentation (7) are given as:

$$\begin{aligned}\mathrm{D}(\cdot) &= (m_{\mathrm{r}} + m_{\mathrm{w}})(I + m_{\mathrm{r}}l^2) - (m_{\mathrm{r}}\cos(x_3(t)))^2, \\ \mathrm{F}_1(\cdot) &= (I + m_{\mathrm{r}}l^2)(m_{\mathrm{r}}lx_4^2(t)\sin(x_3(t)) - k_{\mathrm{T}}x_2(t)) \\ &\quad - (m_{\mathrm{p}}l_{\mathrm{p}} + m_{\mathrm{c}}l_{\mathrm{c}})m_{\mathrm{r}}lg\sin(x_3(t))\cos(x_3(t)), \\ \mathrm{F}_2(\cdot) &= (m_{\mathrm{w}} + m_{\mathrm{r}})g(m_{\mathrm{c}}l_{\mathrm{c}} + m_{\mathrm{p}}l_{\mathrm{p}})\sin(x_3(t)) \\ &\quad - m_{\mathrm{r}}l\cos(x_3(t))(m_{\mathrm{r}}lx_4^2(t)\sin(x_3(t)) - k_{\mathrm{T}}x_2(t)), \\ \mathrm{B}_1(\cdot) &= I + m_{\mathrm{r}}l^2,\ \mathrm{B}_2(\cdot) = \mathrm{G}_1(\cdot) = m_{\mathrm{r}}l\cos(x_3(t)), \\ \mathrm{G}_2(\cdot) &= (m_{\mathrm{w}}l_{\mathrm{c}} + m_{\mathrm{r}}(l_{\mathrm{c}} - l))\cos(x_3(t)),\end{aligned} \tag{8}$$

where $\mathrm{D}(\cdot)$ and $\mathrm{B}_1(\cdot) \neq 0\ \forall t \in \mathbb{T}$.

By invoking to the methodology of control system synthesis presented in [8]–[10], the SMC design must be preceded by performing additional artificial substitution under the control signal $F(t)$ a signal of $F_{\mathrm{SMC}}(t) \in \boldsymbol{\mathcal{F}} \subset \mathbb{R}$. In general, for the pendulum systems, this particular procedure is established by proposing the control signal as one which makes the second differential equation from (7) dependent to only new control

signal $u(t) \in \boldsymbol{\mathcal{U}} \subset \mathbb{R}$, and also makes the fourth differential equation from (7) significantly simplified. Hence, $F_{\mathrm{SMC}}(t)$ can be introduced as:

$$F_{\mathrm{SMC}}(t) = \frac{\mathrm{D}(\cdot)}{\mathrm{B}_1(\cdot)} u(t) - \frac{\mathrm{F}_1(\cdot)}{\mathrm{B}_1(\cdot)}. \tag{9}$$

Moreover, the control signal is bounded due to physical properties of the actuator subsystem, and saturation function is given as: $\mathrm{SAT}_{\mathrm{F}}[\cdot]$ with symmetric saturation – supremum of control signal. Hence, (9) is replaced by:

$$F_{\mathrm{SMC}}^{\mathrm{SAT}}(t) = \mathrm{SAT}_{\mathrm{F}} \left[\frac{\mathrm{D}(\cdot)}{\mathrm{B}_1(\cdot)} u(t) - \frac{\mathrm{F}_1(\cdot)}{\mathrm{B}_1(\cdot)} \right]. \tag{10}$$

However, performing the above–introduced procedure on model (7) leads to a very complicated unserviceable form of the 'new' fourth differential equation. Therefore, cognitive model (7) cannot be directly used for SMC synthesis purposes. In fact, the obtained form of the transformed model can be used in the next steps of synthesis, however; taking into account that the considered SMC must be a robust controller, the whole issue may be solved in an alternative way. It is easy to notice that, the model (7) is very detailed, thus certain simplifications can be performed to effective control system synthesis. Assuming that the mass of load can be neglected, i.e. $m_{\mathrm{c}} = 0$, (4), (5), and (6) take forms:

$$l = l_{\mathrm{p}},\ m_{\mathrm{r}} = m_{\mathrm{p}},\ I = \frac{1}{3} l_{\mathrm{p}}^2 m_{\mathrm{p}}. \tag{11}$$

This involves the possibility of transforming model (7) into simplified version, which not include exact expressions for moment of inertia – I, mass of arm – m_{r}, and distance – l. These parameters are not considered implicitly in the model, since they can be expressed by the other parameters (11). Hence, taking into account the above considerations, (9), and neglecting external disturbance $Z(t)$, the simplified dynamics in affine non–linear form is as follows:

$$\dot{\boldsymbol{x}}(t) = \underbrace{\begin{bmatrix} x_2(t) \\ 0 \\ x_4(t) \\ \dfrac{3g \sin(x_3(t))}{4l} \end{bmatrix}}_{\boldsymbol{f}(\boldsymbol{x}(t))} + \underbrace{\begin{bmatrix} 0 \\ 1 \\ 0 \\ \dfrac{3\cos(x_3(t))}{4l} \end{bmatrix}}_{\boldsymbol{g}(\boldsymbol{x}(t))} u(t), \tag{12}$$

where: $\boldsymbol{f}(\cdot)$ and $\boldsymbol{g}(\cdot)$ are introduced as smooth vector fields which maps $\boldsymbol{\mathcal{X}}$ into $T_{\boldsymbol{x}}\boldsymbol{\mathcal{X}}$.

Model (12) is used as the utility model for SMC synthesis purposes. Also, it is worth adding that, assumption (11) holds for the SU problem.

IV. Synthesis of the control system

In this section, the synthesis of the control system is presented, with the main focus on the design of SMC to stabilise the IP at the upper position.

A. Synthesis of the SMC

The first stage of the SMC synthesis is associated with performing feedback linearisation [14], [19]. This operation is based on coordinate transformation, due to obtaining controllability canonical form of the approximated system's dynamics (12), sliding mode surface, and derivation of non–continuous control law. According to [8]–[10], the classical way of single input performing feedback linearisation cannot be established in this case. It is because, the control distribution calculated by using model (12) is not involutive (near the operating point) at all [15], [19]. Therefore, the method based on using controllable approximate of the original system has been incorporated from [10], [16]. Due to the fact, that the 'output' function $h(\boldsymbol{x}(t))$ related to state coordinate transformation is associated with suspecting the relative degree of the 'output' equal to the dimension of the system, the full state coordinate transformation can be performed. Thus, the new involutive distribution Δ must be calculated by using Lie brackets of the vector fields $\boldsymbol{f}(\cdot)$ and $\boldsymbol{g}(\cdot)$. After that, terms associated with non–zero $\boldsymbol{g}(\cdot)$ related Lie derivatives must be neglected. Hence, the control distribution Δ, which has rank equals three in the neighbourhood of $\boldsymbol{x}_{\mathrm{op}}$ is calculated as follows:

$$\Delta = \mathrm{span}\left\{ \boldsymbol{g}(\cdot),\ [\boldsymbol{f}(\cdot),\ \boldsymbol{g}(\cdot)],\ [\boldsymbol{g}(\cdot),\ [\boldsymbol{f}(\cdot),\ \boldsymbol{g}(\cdot)]] \right\}, \tag{13}$$

where $[\cdot, \cdot]$ denotes the Lie bracket of two vector fields.

By invoking to the Frobenius' theorem, the output function related to (one–dimensional) co–distribution $\mathrm{span}\{dh(\boldsymbol{x}(t))\}$ must be defined as the annihilator of (13) [15], [19]:

$$\mathrm{span}\{dh(\boldsymbol{x}(t))\} = \Delta^{\perp}, \tag{14}$$

where the operator $(\cdot)^{\perp}$ is an annihilator of vector field.

Therefore, by solving the set of three linear, homogenous partial differential equations derived from condition (14), the output function can be proposed as:

$$h(\boldsymbol{x}(t)) = \frac{1}{4} x_1(t) + \frac{1}{3} l \ln \left(\frac{1 + \sin(x_3(t))}{\cos(x_3(t))} \right). \tag{15}$$

The coordinate transformation mapping $\boldsymbol{\Phi}\colon \boldsymbol{x} \to \boldsymbol{\xi}$ must be defined as a local diffeomorphism $\boldsymbol{\Phi}(\mathbf{0}^{\mathrm{n}\times 1}) = \mathbf{0}^{\mathrm{n}\times 1}$, and induces the approximation model of the original simplified model (12) given in controllability canonical form as:

$$\begin{aligned} \dot{\xi}_1(t) &= \xi_2(t) = L_{\boldsymbol{f}} h\left(\boldsymbol{\Phi}^{-\mathbf{1}}(\boldsymbol{\xi})\right), \\ \dot{\xi}_2(t) &= \xi_3(t) = L_{\boldsymbol{f}}^2 h\left(\boldsymbol{\Phi}^{-\mathbf{1}}(\boldsymbol{\xi})\right), \\ \dot{\xi}_3(t) &= \xi_4(t) = L_{\boldsymbol{f}}^3 h\left(\boldsymbol{\Phi}^{-\mathbf{1}}(\boldsymbol{\xi})\right), \\ \dot{\xi}_4(t) &= f_{\xi}(\boldsymbol{x}(t)) + g_{\xi}(\boldsymbol{x}(t)) u(t) \\ &= L_{\boldsymbol{f}}^4 h\left(\boldsymbol{\Phi}^{-\mathbf{1}}(\boldsymbol{\xi})\right) + L_{\boldsymbol{g}} L_{\boldsymbol{f}}^3 h\left(\boldsymbol{\Phi}^{-\mathbf{1}}(\boldsymbol{\xi})\right) u(t), \end{aligned} \tag{16}$$

where $g_{\xi}(\boldsymbol{x}(t)) \neq 0\ \forall t \in \mathbb{T}$ and $f_{\xi}(\boldsymbol{x}(t))$ are scalar functions calculated as subsequent Lie derivatives $L_{(\cdot)}^{(\cdot)}(\cdot)$ of the output function $h(\boldsymbol{x}(t))$.

However, the output function (15) does not induce the relative degree equals the dimension of the system due to the fact, that function $L_{\boldsymbol{g}} L_{\boldsymbol{f}}^2 h = -0.5 x_4(t) \tan(x_3(t))$ is not equal to zero $\forall t \in \mathbb{T}$. Arising of this situation can be claimed

as a consequence of obtaining the involutive distribution Δ. Hence, to perform feedback linearisable form of model (12), by invoking to the methodology presented in [10], [16], [17], indicated component is neglected and the coordinate transformation can be defined as:

$$\begin{aligned}
\Phi_1(\boldsymbol{x}(t)) &= \frac{1}{4}x_1(t) + \frac{1}{3}l\ln\left(\frac{1+\sin(x_3(t))}{\cos(x_3(t))}\right),\\
\Phi_2(\boldsymbol{x}(t)) &= \frac{1}{4}x_2(t) + \frac{lx_4(t)}{3\cos(x_4(t))},\\
\Phi_3(\boldsymbol{x}(t)) &= \frac{4l\sin(x_3(t))x_4^2(t) + 3g\cos(x_3(t))\sin(x_3(t))}{12\cos^2(x_3(t))},\\
\Phi_4(\boldsymbol{x}(t)) &= \frac{8lx_3^3(t) + 9gx_4(t)\cos(x_3(t))}{12\cos^2(x_3(t))}\\
&\quad + \frac{-6gx_4(t)\cos^3(x_3(t)) - 4lx_4^3(t)\cos^2(x_3(t))}{12\cos^2(x_3(t))}.
\end{aligned} \tag{17}$$

By using (17), the non–lienar functions $f_\xi(\boldsymbol{x}(t))$ and $g_\xi(\boldsymbol{x}(t))$ from (16) are calculated as:

$$\begin{aligned}
f_\xi(\boldsymbol{x}(t)) &= \frac{\sin(x_3(t))(96l^2x_3^4(t) + 27g^2\cos^2(x_3(t)))}{48l\cos^4(x_3(t))}\\
&\quad + \frac{\sin(x_3(t))(-16l^2x_3^4(t)\cos^2(x_3(t)))}{48l\cos^4(x_3(t))}\\
&\quad + \frac{\sin(x_3(t))(-36glx_4^2(t)\cos^3(x_3(t)))}{48l\cos^4(x_3(t))}\\
&\quad + \frac{\sin(x_3(t))(144glx_4^2(t)\cos(x_3(t)))}{48l\cos^4(x_3(t))}\\
&\quad + \frac{\sin(x_3(t))(-18g^2\cos^4(x_3(t)))}{48l\cos^4(x_3(t))},\\
g_\xi(\boldsymbol{x}(t)) &= \frac{6g\cos^3(x_3(t)) - 9g\cos(x_3(t)) - 24lx_4^2(t)}{16l\cos^2(x_3(t))}\\
&\quad + \frac{12lx_4^2(t)\cos^2(x_3(t))}{16l\cos^2(x_3(t))}.
\end{aligned} \tag{18}$$

In order to check that the coordinate transformation is the local diffeomorphism near the operating point $\boldsymbol{x}_{\mathrm{op}}$, the Jacobi matrix of the coordinate transformation:

$$\left.\frac{\partial\boldsymbol{\Phi}}{\partial\boldsymbol{x}}\right|_{\boldsymbol{x}(t)=\boldsymbol{x}_{\mathrm{op}}} = \begin{bmatrix} 0.25 & 0 & 0.33l & 0\\ 0 & 0.25 & 0 & 0.33l\\ 0 & 0 & 0.25g & 0\\ 0 & 0 & 0 & 0.25g \end{bmatrix}, \tag{19}$$

must be non–singular. Quadratic Jacobi matrix (19) has a full rank $\forall t \in \mathbb{T}$ due to the fact, that its determinant is equal to $0.0039g^2 > 0$. Hence, the coordinate transformation impose a local diffeomorphism in a neighbourhood of operating point $\boldsymbol{x}_{\mathrm{op}}$, what make feedback linearisation control law applicable.

When the controllability canonical form was obtained, the SMC can be synthesised [14], [19]. Taking into account, that the single input feedback linearisation based SMC is able to track only one dimensional reference signal $y_{\mathrm{d}}(t) \in \boldsymbol{\mathcal{Y}} \subset \mathbb{R}$, the original problem of IP stabilising at $\boldsymbol{x}_{\mathrm{op}}$ must be reformulated in the view of tracking $y_{\mathrm{d}}(t) = \Phi_1(\boldsymbol{x}_{\mathrm{op}}) = 0$. Since the all of the states are controllable, not only full stabilisation of the internal dynamics is possible, but also tracking of the desired trajectories by all of the states. The operating point is equivalent to the upper equilibrium point of the IP internal dynamics, it is only needed to check how the transformed desired signal $y_{\mathrm{d}}(t)$, and its derivatives $y_{\mathrm{d}}^{(1)}(t)$, $y_{\mathrm{d}}^{(2)}(t)$ and $y_{\mathrm{d}}^{(3)}(t)$ behave in time:

$$\left.\boldsymbol{\Phi}(\boldsymbol{x}(t))\right|_{\boldsymbol{x}(t)=\boldsymbol{x}_{\mathrm{op}}} = \begin{bmatrix} y_{\mathrm{d}} & y_{\mathrm{d}}^{(1)} & y_{\mathrm{d}}^{(2)} & y_{\mathrm{d}}^{(3)} \end{bmatrix}^{\mathrm{T}} = \boldsymbol{0}^{4\times 1}. \tag{20}$$

According to the methodology of tracking polynomial control theory [15], all of the derivatives of the $y_{\mathrm{d}}(t)$ are always equal to zero. For the desired trajectory $y_{\mathrm{d}}(t)$, the tracking error is defined as $e(t) \triangleq h(\boldsymbol{x}(t)) - y_{\mathrm{d}}(t)$.

By defining $S = \left\{\boldsymbol{x}(t) \in \boldsymbol{\mathcal{X}} \subset \mathbb{R}^4 \mid s(\boldsymbol{x}(t), t) = 0\right\}$ as a sliding surface which is a proper manifold, the sliding mode variable is introduced as:

$$s(\boldsymbol{x}(t), t) = e^{(3)}(t) + 3\lambda e^{(2)}(t) + 3\lambda^2 e^{(1)}(t) + \lambda^3 e(t), \tag{21}$$

where $(\cdot)^{(\mathrm{der})}(t)$, $\mathrm{der} \in \mathbb{N}_+$ indicates the der degree derivative operator, and $\lambda \in \mathbb{R}_+$ is a tuning parameter which selection is justified in [20].

Thus, by two–sided differentiation of (21):

$$\begin{aligned}
\dot{s}(\boldsymbol{x}(t), t) &= e^{(4)}(t) + 3\lambda e^{(3)}(t) + 3\lambda^2 e^{(2)}(t) + \lambda^3 e^{(1)}(t)\\
&= f_\xi(\boldsymbol{x}(t)) + g_\xi(\boldsymbol{x}(t))u(t) + 3\lambda y^{(3)}(t)\\
&\quad + 3\lambda^2 y^{(2)}(t) + \lambda^3 y^{(1)}(t) = 0,
\end{aligned} \tag{22}$$

the following control law $u(t)$ is obtained:

$$\begin{aligned}
u(t) &\triangleq u_{\mathrm{sw}}(t) + u_{\mathrm{eq}}(t),\\
u_{\mathrm{sw}}(t) &= -K\mathrm{sgn}(s(\boldsymbol{x}(t), t)),\\
u_{\mathrm{eq}}(t) &= \frac{-f_\xi(\boldsymbol{x}(t)) + 3\lambda y^{(3)}(t) + 3\lambda^2 y^{(2)}(t) + \lambda^3 y^{(1)}(t)}{g_\xi(\boldsymbol{x}(t))},
\end{aligned} \tag{23}$$

where: $u_{\mathrm{sw}}(t) \in \boldsymbol{\mathcal{U}} \subset \mathbb{R}$ is non–continuous sliding mode term; $u_{\mathrm{eq}}(t) \in \boldsymbol{\mathcal{U}} \subset \mathbb{R}$ is continuous equivalent control term; $K \in \mathbb{R}_+$ is gain coefficient; $\mathrm{sgn}(\cdot)$ stands for the signum function.

The stability of the devised SMC can be proved by using direct Lyapunov method [14].

For chattering phenomenon avoidance, the signum function from (22) must be replaced by its approximation function [14]. For this purposes, the proposed function is as follows:

$$\mathrm{sign}(s(\boldsymbol{x}(t), t)) \approx \frac{s(\boldsymbol{x}(t), t)}{|s(\boldsymbol{x}(t), t)| + \epsilon}, \tag{24}$$

where $\epsilon \in \mathbb{R}_+$ is a tuning parameter.

B. Synthesis of the SU with SC

The synthesis of the SU with SC controller is based on utilisation of the energy–based approach [2], [10], [11]. The total mechanical energy of angular motion $E(t) \in \mathbb{R}_+$ of the IP in any time $t \in \mathbb{T}$, and the total mechanical energy of angular motion appointed in lower equilibrium point $E(t)\big|_{\boldsymbol{x}_{\mathrm{down}}} \triangleq E_0$ are given as:

$$E(t) = m_{\mathrm{r}}gl\cos(x_3(t)) + 0.5x_4^2(t),\ E_0 = m_{\mathrm{r}}gl. \tag{25}$$

Hence, the swing–up control law $F_{\mathrm{SU}}(t) \in \boldsymbol{\mathcal{F}} \subset \mathbb{R}$ and its saturated version $F_{\mathrm{SU}}^{\mathrm{SAT}}(t) \in \boldsymbol{\mathcal{F}} \subset \mathbb{R}$ are defined as [2]:

$$\begin{aligned} F_{\mathrm{SU}}(t) &= k_{\mathrm{SU}}(E(t) - E_0)\mathrm{sign}(x_4(t)\cos(x_3(t))), \\ F_{\mathrm{SU}}^{\mathrm{SAT}}(t) &= \mathrm{SAT}_{\mathrm{F}}\left[F_{\mathrm{SU}}(t)\right], \end{aligned} \tag{26}$$

where $k_{\mathrm{SU}} > 0$ signifies the swing–up mechanism parameter.

To guarantee proper action of the entire (SMC–SU–SC) control system, the switching condition must include not only the performance of the robust SMC and SU regulators but also some physical constraints of control signal $F(t)$. Thus, to establish the operating regions of both SMC and SU, the analysis of $h(\boldsymbol{x}(t))$ function is performed. Taking into account that, a significant part of $h(\boldsymbol{x}(t))$ is based on natural logarithm function, the interior of $\ln(\cdot)$ from (15) must be bigger than zero $\forall t \in \mathbb{T}$. Further considering that for the IP stabilisation at the upper position, the third state variable must be contained in $x_3(t) \in \Omega_1 = [-\pi, \pi] \subset \boldsymbol{\mathcal{X}}$, the new set $\Omega_2 \subset \boldsymbol{\mathcal{X}}$ is introduced as $\Omega_2 = \{x_3(t) \in \Omega_1 \mid \cos(x_3(t)) \neq 0\} = \{-0.5\pi; 0.5\pi\}$. By taking interior function of $\ln(\cdot)$ from (15), the following inequalities are derived:

$$\begin{aligned} (1 + \sin(x_3(t)))/(\cos(x_3(t))) > 0 \;\big|\cdot (\cos(x_3(t)))^2, \\ \sin(x_3(t))\cos(x_3(t)) > -\cos(x_3(t)), \\ \sin(2x_3(t)) > -2\cos(x_3(t)). \end{aligned} \tag{27}$$

Assuming that the potential solutions of (27) are contained in $\Omega_1 \setminus \Omega_2$, the potential operating region must be $\Omega_3 = (-0.5\pi, 0.5\pi) \subset \Omega_1$. Hence, taking into account potential constraints on the SU performance, the final operating region Ω_{SMC} must be established as contained in Ω_3. Thus, based on experimental results, the SC is determined as:

$$F(t) = \begin{cases} F_{\mathrm{SMC}}(t) & \text{for } |x_3(t)| < \Psi \\ F_{\mathrm{SU}}(t) & \text{for } |x_3(t)| \geq \Psi \end{cases}, \tag{28}$$

where angle Ψ has been determined as $\Psi = \pi/6$ [rad].

Hence, for $x_3(t)$ operating regions of SMC and SU regulators are as follows: $\Omega_{\mathrm{SMC}} = (-\Psi, \Psi) \subset \boldsymbol{\mathcal{X}}$, $\Omega_{\mathrm{SU}} = [-\Psi, -\pi) \cup [\Psi, \pi) \subset \boldsymbol{\mathcal{X}}$.

Remark 1. As it has been mentioned in previous sections, the entire control system includes not only SMC–SU–SC, but also important subsystems of actuator and measuring device (see [2]). Taking into account that, the performance of both subsystems is sufficient, the developed solution is feasible to implement in a real plant, as confirmed by the simulation studies in the next section.

V. Simulation Results

The devised control system has been implemented in Matlab/Simulink environment. The values of the main parameters of the IP are as follows: $m_{\mathrm{w}} = 0.762$ [kg], $m_{\mathrm{p}} = 0.178$ [kg], $l_{\mathrm{p}} = 0.18$ [m], and $k_{\mathrm{T}} = 7.5$ [Ns/m]. Both these values and the implemented subsystems of the actuator and measuring device have been taken from [2]. In turn, the selected values of the parameters of the designed control system are as follows: $K = 5$, $\lambda = 5$, $\epsilon = 0.1$, and $k_{\mathrm{SU}} = 20$. These have been supplemented with $\mathrm{SAT}_{\mathrm{F}}[\cdot] = 7$ [N] and the load mass of 0 and 0.1 [kg] during experiments 1 and 2, respectively.

The simulation results for experiment 1 are presented in Fig. 2. As can be noticed, after about 5 [s] the IP arm has been stabilised at the upper position and the cart is in the middle of the gantry. Moreover, this effect is obtained with control signals respecting the saturation value – for comparison, Fig. 2a shows the trajectories of control signals without saturation. In addition, fulfilling the control goal required about 0.4 [m] of the gantry, which meets the technological constraints of the plant (the length of gantry equals 1 [m] – see [2]).

The second experiment tested the robustness of the control system, i.e. the ability to reject external disturbance $Z(t)$ and the robustness to uncertainty in the parameters – change in mass m_{c}. The results obtained are given in Fig. 3. They show that the control performance is maintained, thus the designed control system meets the requirements imposed on it.

VI. Conclusions

In this paper, the control problem of an inverted pendulum on a cart has been investigated. The devised control system

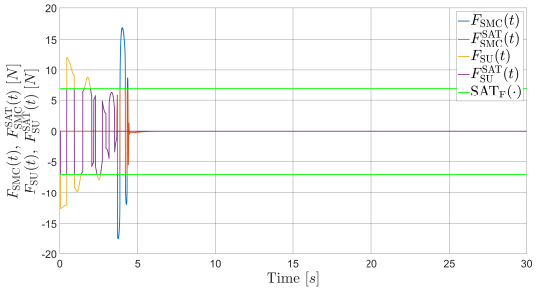

(a) Trajectories of control signals - experiment 1

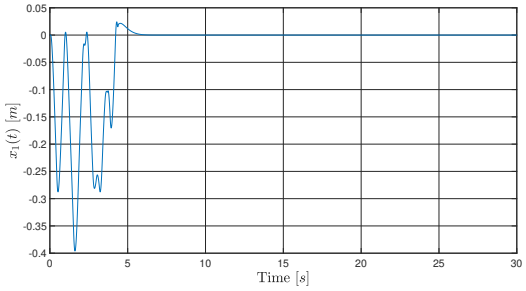

(b) Trajectory of $x_1(t)$ - experiment 1

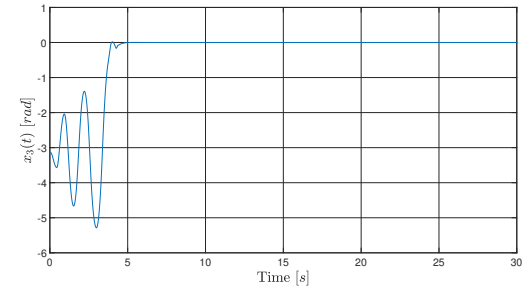

(c) Trajectory of $x_3(t)$ - experiment 1

Fig. 2. Trajectories of control signals and state variables - experiment 1.

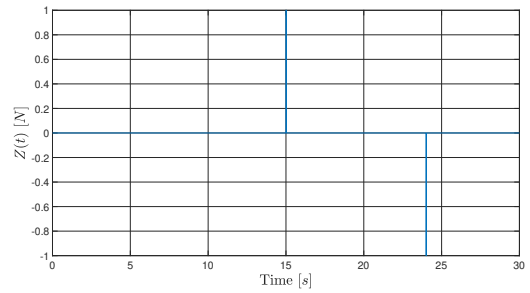

(a) Trajectory of $Z(t)$ - experiment 2

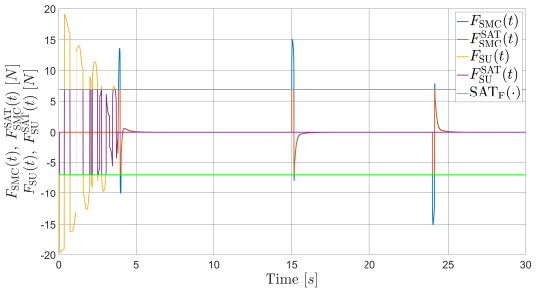

(b) Trajectories of control signals - experiment 2

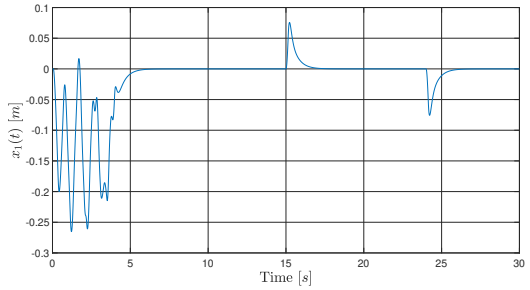

(c) Trajectory of $x_1(t)$ - experiment 2

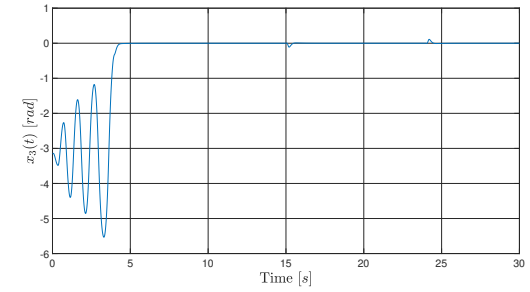

(d) Trajectory of $x_3(t)$ - experiment 2

Fig. 3. Trajectories of control signals, external disturbance and state variables - experiment 2.

includes the sliding mode controller for stabilisation of the inverted pendulum at the upper equilibrium point and the energy–based swing–up mechanism bringing the pendulum arm to the neighbourhood of this point with switching condition between regulators. The designed control system allows external disturbance rejection and coping with uncertainty in parameters as well as respects the technological constraints of the real plant. The efficiency of this structure has been discussed and analysed by performing proper simulations in Matlab/Simulink environment.

ACKNOWLEDGEMENTS

The research work was done in accordance with funding from Polish MEiN under Young Researcher Support Program. The authors wish to express their thanks for support.

REFERENCES

[1] K. Andrzejewski, M. Czyżniewski, M. Zielonka, R. Łangowski, and T. Zubowicz, "A comprehensive approach to double inverted pendulum modelling," *Archives of Control Sciences*, vol. 29, no. 3, pp. 459–483, 2019.

[2] M. Waszak and R. Łangowski, "An automatic self-tuning control system design for an inverted pendulum," *IEEE Access*, vol. 8, pp. 26 726–26 738, 2020.

[3] L. B. Prasad, B. Tyagi, and H. O. Gupta, "Optimal control of nonlinear inverted pendulum dynamical system with disturbance input using PID controller and LQR," in *Proceedings of the IEEE International Conference on Control System, Computing and Engineering*, 2011, pp. 540–545.

[4] J.-J. Wang, "Simulation studies of inverted pendulum based on PID controllers," *Simulation Modelling Practice and Theory*, vol. 19, no. 1, pp. 440–449, 2011.

[5] C. Mahapatra and S. Chauhan, "Tracking control of inverted pendulum on a cart with disturbance using pole placement and LQR," in *Proceedings of the International Conference on Emerging Trends in Computing and Communication Technologies*, 2017, pp. 1–6.

[6] S. Trimpe, A. Millane, S. Doessegger, and R. D'Andrea, "A self-tuning LQR approach demonstrated on an inverted pendulum," in *Proceedings of 19th IFAC World Congress*, 2014, pp. 11 281–11 287.

[7] M.-S. Park and D. Chwa, "Swing-up and stabilization control of inverted-pendulum systems via coupled sliding-mode control method," *IEEE Transactions on Industrial Electronics*, vol. 56, pp. 3541–3555, 2009.

[8] S. Mahjoub, F. Mnif, and N. Derbel, "Second-order sliding mode control applied to inverted pendulum," in *14th International Conference on Sciences and Techniques of Automatic Control Computer Engineering - STA'2013*, 2013, pp. 269–273.

[9] S. Irfan, A. Mehmood, M. Tayyab Razzaq, and J. Iqbal, "Advanced sliding mode control techniques for inverted pendulum: Modelling and simulation," *Engineering Science and Technology, an International Journal*, vol. 21, no. 4, pp. 753–759, 2018.

[10] A. Aguilar, "Approximate feedback linearization and sliding mode control for the single inverted pendulum," Queen's University, Mathematics and Engineering, 2002.

[11] J. Lee, R. Mukherjee, and H. K. Khalil, "Output feedback stabilization of inverted pendulum on a cart in the presence of uncertainties," *Automatica*, vol. 54, pp. 146–157, 2015.

[12] A. I. Roose, S. Yahya, and H. Al-Rizzo, "Fuzzy-logic control of an inverted pendulum on a cart," *Computers and Electrical Engineering*, vol. 61, pp. 31–47, 2017.

[13] Z. Li and C. Yang, "Neural-adaptive output feedback control of a class of transportation vehicles based on wheeled inverted pendulum models," *IEEE Transactions on Control Systems Technology*, vol. 20, no. 6, pp. 1583–1591, 2012.

[14] V. I. Utkin, *Sliding modes in control and optimization*. Berlin, Germany: Springer-Verlag, 1992.

[15] A. Isidori, *Nonlinear control systems*. London, UK: Springer-Verlag, 1995.

[16] J. Hauser, S. Sastry, and P. Kokotović, "Nonlinear control via approximate input-output linearization: the ball and beam example," *IEEE Transactions on Automatic Control*, vol. 37, no. 3, pp. 392–398, 1992.

[17] D. A. Voytsekhovsky and R. M. Hirschorn, "Stabilization of single-input nonlinear systems using higher order compensating sliding mode control," in *Proceedings of the 44th IEEE Conference on Decision and Control*, 2005, pp. 566–571.

[18] R. P. M. Chan, K. A. Stol, and C. R. Halkyard, "Review of modelling and control of two–wheeled robots," *Annual Reviews in Control*, vol. 37, no. 1, pp. 89–103, 2013.

[19] N. Nijmeijer and A. J. Van der Schaft, *Nonlinear dynamical control systems*. New York, US: Springer-Verlag, 1990.

[20] J.-J. E. Slotine and W. Li, *Applied nonlinear control*. Englewood Cliffs, NJ, US: Prentice Hall, 1991.